Molecular Vision 2014; 20:441-457 <http://www.molvis.org/molvis/v20/441>
Received 4 September 2013 | Accepted 28 March 2014 | Published 30 March 2014

Hypoxia-inducible factor-1α, von Hippel-Lindau protein, and heat shock protein expression in ophthalmic pterygium and normal conjunctiva

Dionysios Pagoulatos,[1] Nikolaos Pharmakakis,[2] John Lakoumentas,[3] Martha Assimakopoulou[1]

[1]Department of Anatomy-Histology and Embryology, School of Medicine, University of Patras, Rion, Greece; [2]Department of Ophthalmology, School of Medicine, University of Patras, Rion, Greece; [3]Department of Medical Physics, School of Medicine, University of Patras, Rion, Greece

Purpose: Enhanced expression of transcription factor hypoxia inducible factor HIF-1α is known to play a critical role in the modulation of cell metabolism and survival pathways as well as having stem-cell–like properties. Furthermore, accumulated data reveal the existence of cross-regulation between the oxygen-sensing and heat shock pathways contributing to the adaptation of cells under stressful conditions. Pterygium, a stem cell disorder with premalignant features, has been reported to demonstrate hypoxia. The purpose of this study was to investigate the co-expression patterns of transcription factor HIF-1α and von Hippel Lindau protein (pVHL)—which normally acts to keep levels of HIF-1α activity low under normoxic conditions—in pterygium and normal conjunctival human samples. Additionally, expression of HIF-1α compared to the activation of heat shock proteins (Hsp90, Hsp70, and Hsp27) was studied. Emphasis was placed on the detection of HIF-1α and Hsp90, which associates with and stabilizes HIF-1α to promote its transcriptional activity.
Methods: Semi-serial paraffin-embedded sections and tissue extracts from pterygium and normal conjunctival samples were studied by immunohistochemistry and western blot analysis, respectively, with the use of specific antibodies. Double labeling immunofluorescence studies on cryostat sections were also included.
Results: Statistically significant increased expression of HIF-1α and Hsps (Hsp90, Hsp70, and Hsp27) in pterygia compared to normal conjunctiva was demonstrated ($p<0.05$). In contrast, no significant difference was detected for pVHL expression ($p>0.05$). Immunohistochemical findings revealed nuclear HIF-1α immunoreactivity in all the epithelial layers of 23/32 (71.8%) pterygium tissues. Furthermore, all epithelial layers of the majority (75%) of pterygium samples showed strong cytoplasmic immunoreactivity for Hsp27 while Hsp27 expression was detected in all pterygia (100%) examined. Hsp27 expression was not observed in the superficial layer of goblet cells. In some samples, focal basal epithelial cells exhibited weak Hsp27 expression or were Hsp27 immunonegative. Immunoreactivity of phopsho-Hsp27 showed the same distribution pattern as Hsp27 did. Epithelium of all pterygia (100%) displayed moderate to strong Hsp90 cytoplasmic immunoreactivity. Furthermore, the majority of pterygia, specifically, 30/32 (93.7%) and 27/32 (84.3%) demonstrated, respectively, Hsp70 and pVHL cytoplasmic immunoreactivity. Hsp90, Hsp70, and pVHL immunoreactivity was mainly detected in basal and suprabasal epithelial layers even though strong immunoreactivity in all epithelial layers was also observed in some pterygia. Stroma vessels were immunopositive for Hsps (Hsp90, Hsp70, and Hsp27) and pVHL. A statistically significant correlation between the expression of HIF-1α and the activation status of Hsps (Hsp90, Hsp70, and Hsp27; $p<0.05$) was observed whereas HIF-1α expression did not correlate with pVHL expression ($p>0.05$). Double labeling immunofluorescence studies showed nuclear HIF-1α co-localization with cytoplasmic Hsp90 expression in cells distributed in the entire epithelium of pterygia, in contrast to, normal conjunctiva, which exhibited only a few scattered epithelial cells with cytoplasmic HIF-1α expression and basal epithelial cells with Hsp90 expression.
Conclusions: The upregulation of coordinated activation of HIF-1α and Hsps in pterygium may represent an adaptive process for the survival of cells under stressful conditions. The significance of the association of HIF-1α with Hsp90 with respect to the therapeutic approach of pterygium requires further evaluation.

Pterygium, derived from the Greek word *πτέρυξ*, meaning "wing," refers to a disorder of the ocular surface that occurs in people throughout the world, especially in countries with prolonged sunshine and a warm climate [1]. The lesion appears as a triangular overgrowth of (in most cases) nasal but also (occasionally) the temporal bulbar conjunctiva on the cornea that may eventually obstruct the visual axis [2]. Histopathological findings demonstrate epithelial changes such as squamous metaplasia and goblet cell hyperplasia [3] and elastotic degenerated connective tissue [4] with prominent neovascularization [5-7] accompanied by an inflammatory cell infiltration [8].

Although there is no consensus on the pathogenesis of pterygium [9,10], ultraviolet radiation is considered to be the

Correspondence to: Martha Assimakopoulou, Department of Anatomy-Histology and Embryology, School of Medicine, University of Patras, Gr-26504 Rion, Greece; Phone: 302610969186; FAX: 302610969178; email: massim@upatras.gr

principal environmental factor that affects epithelial stem cells residing at the nasal limbus [11,12]. According to a recent report, pterygium is likely a stem cell disorder with premalignant features [13]. Although pterygium was traditionally recognized as a benign lesion, studies indicate that it is associated with cancers of the ocular surface such as squamous cell carcinoma and malignant melanoma [14-16]. Furthermore, fibroblasts isolated from human pterygia exhibit transformed cell characteristics showing a possible preneoplastic nature in the pterygium outgrowth [17]. Epithelial-mesenchymal transition (EMT), a phenomenon that occurs during oncogenesis [18], has been proposed as a mechanism for the origin of pterygial fibroblasts [19]. Additionally, pterygium is characterized by local invasiveness [12,20,21] and a high recurrence rate [22]. Recent clinicopathological analysis implies that neovascularization of pterygia is triggered by ocular hypoxia [23]. Additionally, EpoR, which is upregulated by ischemia or hypoxia, is increased in pterygium [24].

A hypoxic microenvironment activates critical signaling pathways in order for cells to overcome the limited availability of nutrients and oxygen. Hypoxia-inducible factors (HIFs) are transcription factors of the basic helix-loop-helix (bHLH)/PAS family, which plays a key role in adaptive cellular responses to hypoxia. HIFs include HIF-1α, which is expressed differently in most tissues, and HIF-2α, which shows a more restricted tissue expression pattern [25,26]. HIF-1α—the oxygen sensitive subunit of hypoxia-inducible factor-1 (HIF-1)—regulates the transcription of numerous target genes involved in energy metabolism, angiogenesis and apoptosis [27]. In normoxic cells, this protein is expressed at extremely low levels due to degradation by the von Hippel Lindau protein (pVHL) [28], a tumor suppressor protein [29,30]. Under hypoxic conditions, the stabilization and activation of HIF-1α is the result of the inability of pVHL to associate with and ubiquinate HIF-1α [31]. However, data show that Hsp90 associates with HIF-1α, resulting in stabilization of HIF-1α [32]. It has been reported that Hsp90 inhibitors, such as geldanamycin and 17-allylaminogeldanamycin (17-AAG), block the binding of Hsp90 to HIF-1α, leading to increased ubiquitination and degradation of HIF-1α [33-35] in hypoxic conditions. Interestingly, the induction of Hsps is HIF dependent. Particularly, heat shock factor (HSF) transcription is upregulated during hypoxia due to direct binding of HIF-1 to HIF-1 response elements in an HSF intron [36,37].

Furthermore, overexpression of Hsps has been observed in response to a wide variety of stress conditions including heat shock [38], radiation [39], viral infection [40], oxidative stress [41], and inflammation as well as ischemia [42]. Hsps are also induced at specific stages of development, differentiation [43], and malignant transformation [44]. Hsps display strong cytoprotective effects by playing the role of molecular chaperones for numerous clients and signaling proteins involved in mechanisms promoting cell survival [45,46]. Hsp90, its client protein Hsp70, and Hsp27 are the dominantly expressed heat shock proteins after different kinds of stress [45,47]. The elevated levels of these proteins in a wide range of human cancers provide prognostic and predictive implications [48].

In this study, we examined the co-expression patterns of transcription factor HIF-1α and pVHL in pterygium and normal conjunctival human samples. In addition, the expression of HIF-1α compared to the expression levels of Hsps (Hsp90, Hsp70, and Hsp27) was studied.

METHODS

Patients: Fifty-four patients with primary or recurrent pterygia who underwent routine pterygium excision surgery in the Department of Ophthalmology, University Hospital Patras, Greece, from 2008 through 2010 were included in this study. Normal bulbar conjunctival tissues (n = 18, mean age 72) from patients undergoing glaucoma or cataract surgery were collected from the same department during the same period. The study population was of Greek origin. Use of the human specimens was in accordance with the University Ethics Commission. All research protocols were conducted, and patients were treated in accordance with the tenets of the Declaration of Helsinki. Clinicodemographic features regarding the study population are presented in Table 1.

Immunohistochemistry: All tissues for immunohistochemistry were fixed in formalin and embedded in paraffin. Consecutive (semi-serial) 4 μm sections of ocular pterygium and normal conjunctival tissue samples were collected on poly-L-lysine coated slides. Pterygia were oriented such that sections were cut longitudinally through the head and the body of the pterygium. One section for each sample was stained with hematoxylin and eosin (H&E). For immunohistochemical studies, the histological sections were deparaffinized in xylene and rehydrated in graded alcohols up to water. Antigen retrieval was performed either by microwaving the slides in 0.01 M citrate buffer (pH 6) for antibodies against pVHL and Hsps (Hsp90, Hsp70, Hsp27, and phosphorylated Hsp27 [phospho-Hsp27 (Ser 82)]) or incubating them with pepsin at 37 °C for 15min for the antibody against HIF-1α. Endogenous peroxidase activity was quenched by treatment with 1% hydrogen peroxide for 20 min. Incubation with an appropriate protein blocking solution was performed. Sections were subsequently incubated with primary antibodies (Table 2). Detection was performed

Table 1. Clinical and demographic characteristics for patients with pterygium included in this study according to the method used for the evaluation of HIF-1a, pVHL, and Hsps.

Variable	IHC	IF	WB
Population (no. of cases)	32	10	12
Age(years)	72.48±11.2	71±7.40	72±8.32
Mean±Standard deviation range	41–88	51–75	50–80
Gender (no. ofcases) Male/Female	22/10	7/3	7/5
Grade (no. of cases) Grade I /Grade II	10/22	4/6	7/5
Location of lesion (no. of cases) Nasal /Temporal	29/3	10/-	12/-
Type of lesion (no. of cases) Primary /Recurrent	27/5	10/-	12/-

IHC: Immunohistochemistry, IF: Immunofluorescense, WB: western blotting

using the Envision Plus Detection System kit, according to the manufacturer's instructions (DakoCytomation, DAKO, Carpinteria, CA), with 3,3′-diaminobenzidine (DAB) as a chromogen, which yielded brown reaction products. Sections were counterstained with Mayer's hematoxylin solution, dehydrated, and mounted. To ensure antibody specificity, negative controls included the omission of primary antibody and substitution with non-immune serum. Control slides were invariably negative for immunostaining. As positive controls, cancer specimens known to express HIF-1α, pVHL, and Hsps were used. Optimal conditions (dilutions, incubation time, and protein blocking) for reproducible results with each primary antibody are shown in Table 2.

Two observers independently evaluated the results of immunohistochemistry in epithelium. Interobserver agreement for evaluation of immunostaining was within 15% (Cohen's kappa = 0.82) [49]. To determine the labeling index (% labeled cells) for each antibody, two observers independently assessed ten non-overlapping, random fields (X400 total magnification) for each case and manually counted 100 epithelial cells in each field with the aid of an ocular grid. Immunopositive endothelial and stromal cells were excluded from the cell counts. Expression of proteins included in this study was examined in adjacent (semi-serial) sections of each sample [50]. Microphotographs were obtained using a Nikon DXM 1200C digital camera mounted on a Nikon Eclipse 80i microscope and ACT-1C software (Nikon Instruments Inc., Melville, NY).

Immunofluorescence: For the double labeling immunofluorescence studies, pterygium and normal conjunctiva frozen samples were embedded in optimum cutting temperature (OCT) compound (BDH, Poole, UK) and cryosectioned at a thickness of 10µ. The sections were post fixed with 4% PFA for 15 min at RT, washed with PBS and 0.3% Triton-X 100 in PBS. After incubation for at least 1 h with blocking solution (0.1% Tween-20 in PBS, 10% fetal bovine serum, and 3% BSA [BSA, Sigma]), sections were labeled overnight at 4 °C with the following primary antibodies mixed

Table 2. Primary antibodies used for Immunohistochemistry, Immunofluorescense and western blotting.

Antibody	Type	Source	Dilution IHC/ IF	WB	Protein blocking	Incubation conditions
HIF-1α clone H1αlpha67	Monoclonal mouse	Novus Biologicals	1:25	1:500	TBS/BSA 3%	ON 4 °C
pVHL clone (52A11)	Monoclonal mouse	Acris Antibodies	1:100	1:500	TBS/BSA 5%	ON 4 °C
Hsp90	Monoclonal rabbit	Cell Signaling	1:250	1:1,000	TBS/BSA 10%	ON 4 °C
Hsp70	Polyclonal rabbit	Cell Signaling	1:100	1:500	TBS/BSA 7%	ON 4 °C
Hsp27	Monoclonal mouse	Biogenex	1:80 1:50	1:1,000	TBS/BSA 2%	ON 4 °C
Phospho-Hsp27 (Ser 82)	Polyclonal rabbit	Cell Signaling		1:1,000	TBS/BSA 5%	ON 4 °C
β-tubulin	Monoclonal mouse	Sigma		1:2,000	5% nonfat milk	ON 4 °C

IHC: Immunohistochemistry, IF: Immunofluorescense, WB: Western Blotting, TBS: Tris-Buffered Saline, BSA: BSA, ON: Overnight

together in blocking solution: HIF-1α and Hsp90. The same dilutions that applied in immunohistochemistry were used (Table 2). After being washed, sections were incubated at room temperature (RT) for 1 h with secondary antibodies Alexa Fluor 488 and 568 goat anti-mouse and anti-rabbit (1/500 and 1/500 respectively; Molecular Probes–Invitrogen, Paisley, UK). The specificity of the staining was determined by omitting the primary antibodies, and 4,6-diamidino-2-phenylindole (DAPI) was used to label cell nuclei. Slides were coverslipped using an aqueous-based mounting medium (Vectashield Hard Set; Vector Laboratories, Burlingame, CA). In addition, double immunofluorescence was performed on deparaffinized sections following the same procedure as described above. Photos were taken with a Nikon Eclipse TE2000-U microscope and collected with the Nikon camera Digital Sight DS-L1 (Nikon, Tokyo, Japan). All images were processed with Adobe Photoshop software (Adobe Systems, San Jose, CA).

Western blotting: After the clinical samples were resected, they were placed immediately on dry ice and stored at −80 °C. Before western blotting, tissue sections were cut onto glass slides and stained following the routine staining protocol. The remainder of the sample was directly transferred into a reaction tube followed by solubilization of the tissue in 100 µl 1% SDS w/v with 4 µl Sigma Phosphatase Inhibitor Cocktail I, 4 µl Sigma Phosphatase Inhibitor Cocktail II, and 4 µl Sigma Protease Inhibitor Cocktail, sonicated, and boiled for 15 min. Protein concentration was measured for each sample by with a BSA protein kit (Pierce, Rockford, IL) and spectrophotometry. Duplicate samples (50 µg of total protein) were separated on 7% (for HIF-1α and Hsp90) and 12% (for pVHL, Hsp70, Hsp27, and phospho-Hsp27) polyacrylamide gel and then transferred on nitrocellulose membranes. Non-specific binding sites were blocked for 1 h with 10% nonfat dried milk at RT. The blots were probed with the primary antibodies at appropriate dilutions (Table 2) and incubated overnight at 4°C. The blots were rinsed with Tris buffered saline (TBS)-Tween and then incubated with goat anti-rabbit horseradish peroxidase-linked immunoglobulin G (IgG) or goat anti-mouse horseradish peroxidase-linked IgG for 1 h at RT. After rinsing, immunoreactive bands were visualized with an enhanced chemiluminescence detection system (ECL, Amersham International, Cardiff, UK). Molecular masses were determined by comparison with protein molecular weight marker standards from Biomol. To ensure equal protein loading, membranes were stripped and reprobed with β-tubulin monoclonal antibody (1:2,000 dilution; Sigma, St. Louis, MO). The blots obtained from at least three independent experiments were analyzed. Luminescence from the blots was detected by exposing the membranes to Fuji-Hyperfilm for 1 to 10 min, to ensure operation within the linear range of the film, followed by digital scanning of the developed film in transparency mode. The scanned image of the membranes and band intensities were calibrated and quantified using NIH ImageJ software (version 1.61).

Statistical analysis: Parametric statistical tests depended on the assumption that data are sampled from a normal (Gaussian) distribution. Testing composite normality was performed using the Shapiro-Wilk W test (along with the Shapiro-Francia correction for leptokurtic samples), when data were not large-sized (<2000). In case of scale data, mean comparisons were performed using the Student *t* test (for bipartite comparisons) and one-way ANOVA (for multi-partite comparisons). Otherwise, median comparisons were performed with non-parametric Wilcoxon's Rank-Sum test (equivalent to the Mann-Whitney U test) and the Kruskal-Wallis test, respectively. Associations of categorical (nominal or ordinal) data were examined using Pearson's Chi-Square test of independence (or the z-test for bipartite proportion comparisons). Correlation analysis of parametric data was performed using Pearson's linear correlation, while the analysis of non-parametric data was performed using Kendall's τ (or Spearman's ρ) rank correlation. In either case, a line to fit data (in a least-squares sense) was generated. In all statistical tests, the significance level was defined as $p<0.05$. Statistical analysis was implemented in MATLAB, release 7.12 (R2011a), using the Statistics Toolbox.

RESULTS

Immunoreactivity for HIF-1α, pVHL, and Hsps in pterygium and normal conjunctival tissue samples: Immunohistochemical analysis showed expression of HIF-1α, pVHL, and Hsps with distinct patterns of cellular localization in the epithelium of pterygium and normal conjunctival samples included in this study. Furthermore, in the pterygium stroma, vascular endothelial cells showed cytoplasmic immunoreactivity for Hsps (Hsp90, Hsp70, and Hsp27) and pVHL. The immunohistochemical data are shown in Figure 1, Figure 2, Figure 3, Figure 4, Figure 5, and Figure 6 and are summarized in Table 3. Nuclear immunoreactivity for HIF-1α was detectable in all the epithelial layers of 23/32 (71.8%) pterygium tissues (Figure 1A). In some cases, cytoplasmic immunoreactivity was also noted (Figure 1B,C,E). Only the nuclear immunoreactivity was taken into consideration during the evaluation of staining. Hsp27 expression was detected in all the pterygia (100%) examined. Furthermore, the majority (75%) of pterygium samples exhibited strong cytoplasmic immunoreactivity for Hsp27 in all epithelial layers (Figure 2A-C). In some samples (about 1%), focal basal cells exhibited

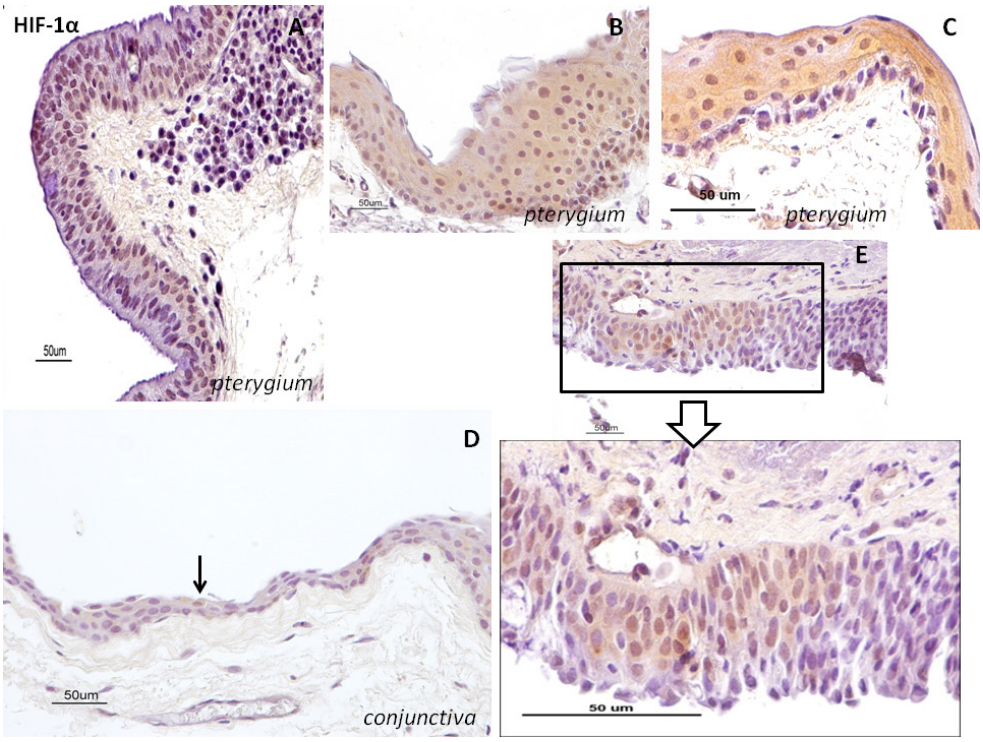

Figure 1. Panel depicting the cellular distribution of HIF-1α in pterygia (**A-C**,**E**) and normal conjunctiva (**D**). **A**: Strong nuclear immunoreactivity in numerous epithelial cells of pterygium. **B**: Strong nuclear and cytoplasmic immunoreactivity in all epithelial layers of pterygium sample. **C**: The basal epithelial cells are HIF-1α negative whereas the remaining cells display nuclear and cytoplasmic immunoreactivity in this pterygium sample. **D**: Arrow indicates a single cell with weak cytoplasmic immunoreactivity for HIF-1α in normal conjunctival epithelium. **E**: HIF-1α positive cells, with nuclear and cytoplasmic immunoreactivity, are adjacent to HIF-1α negative cells, highlighting the staining heterogeneity within individual tissues. (Dako Envision Plus Detection System with hematoxylin counterstain, original magnification X400, bar 50 µm).

weak Hsp27 expression or were Hsp27-negative (Figure 2C). Hsp27 expression was not observed in the superficial layer of goblet cells (Figure 3A). Immunoreactivity of phospho-Hsp27 showed the same distribution pattern as Hsp27 did. Additionally, all pterygia (100%) showed moderate to strong cytoplasmic immunoreactivity for Hsp90, mainly in basal and suprabasal cells (Figure 3B) although Hsp90 immunoreactivity was detected occasionally in almost all epithelial layers (Figure 4A-C). Furthermore, basal and suprabasal cells displayed moderate cytoplasmic immunoreactivity for Hsp70 in 30/32 (93.7%) pterygia (Figure 3C, Figure 5A,B). In some samples, however, Hsp70 immunoreactivity was observed in the entire epithelium (Figure 5C,D). Occasionally, strong immunoexpression of Hsp70 in basal cells was detected (Figure 5D). Weak pVHL immunoreactivity was detected in 27/32 (84.3%) of pterygia whereas moderate to strong pVHL immunoreactivity, particularly in basal and suprabasal cells, was also noted (Figure 6A,B). In some samples, pVHL-expressing cells with strong immunoreactivity were distributed in all epithelial layers (Figure 3D, Figure 6C). In the pterygia included in this study, there was considerable staining heterogeneity among different samples concerning the HIF-1α, Hsps, and pVHL immunostaining. Furthermore, variability of positive cells was also common within individual tissues.

Quantitative analyses of the immunohistochemical labeling indices (LIs) showed no significant differences based on age, gender, or grade of pterygium ($p>0.05$). However, there were significant correlations between the LIs for HIF-1α and all three Hsps (Figure 7A-C) but not between HIF-1α and pVHL (Figure 7F). Furthermore, there were significant correlations between the LIs for pVHL and Hsp90, as well as, between pVHL and Hsp70 (Figure 7D,E) but not between pVHL and Hsp27 ($p = 0.06$). The expression of each Hsp was significantly correlated with the other Hsps (Figure 8).

In normal conjunctival epithelium, a small number of epithelial conjunctival cells showed nuclear HIF-1α immunoreactivity although in some samples both nuclear and cytoplasmic staining were observed. Intense cytoplasmic immunoreactivity was observed for Hsp27 mainly in basal and suprabasal layers of all samples. Furthermore, Hsp90, Hsp70, and pVHL expression was observed in basal and suprabasal epithelial cells that showed weaker immunoreactivity compared to the pterygia (Figure 1, Figure 2, Figure 4, Figure 5, and Figure 6). Considerable staining heterogeneity of the Hsps and pVHL was observed among and within conjunctival samples. Comparison of mean labeling indices (MLIs) between primary and recurrent pterygia showed a

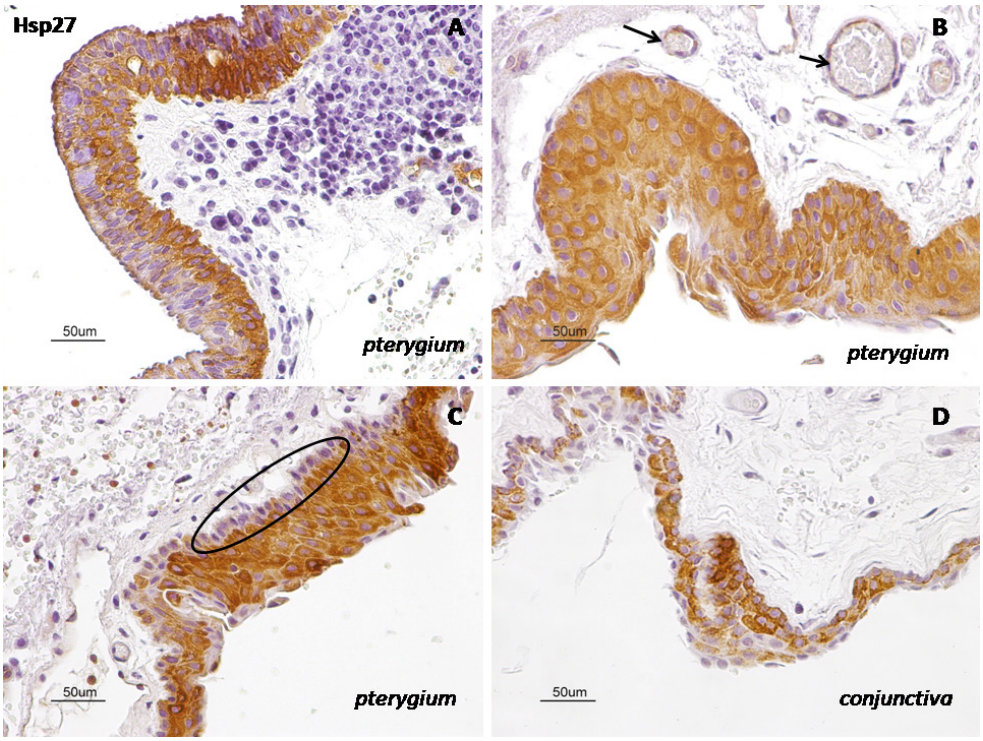

Figure 2. Panel depicting the cellular distribution of Hsp27 in pterygia (**A**-**C**) and normal conjunctiva (**D**). **A, B**: Strong cytoplasmic immunoreactivity in high percentage of epithelial cells. **B**: Arrows indicate vessels in pterygium stroma that are Hsp27 positive. **C**: Oval indicates Hsp27-negative basal cells whereas the entire epithelium exhibits extensive Hsp27 immunoreactivity. **D**: A representative normal conjunctival sample with intense cytoplasmic Hsp27 immunoreactivity mostly in basal and suprabasal cells. (Dako Envision Plus Detection System with hematoxylin counterstain, original magnification X400, bar 50 µm).

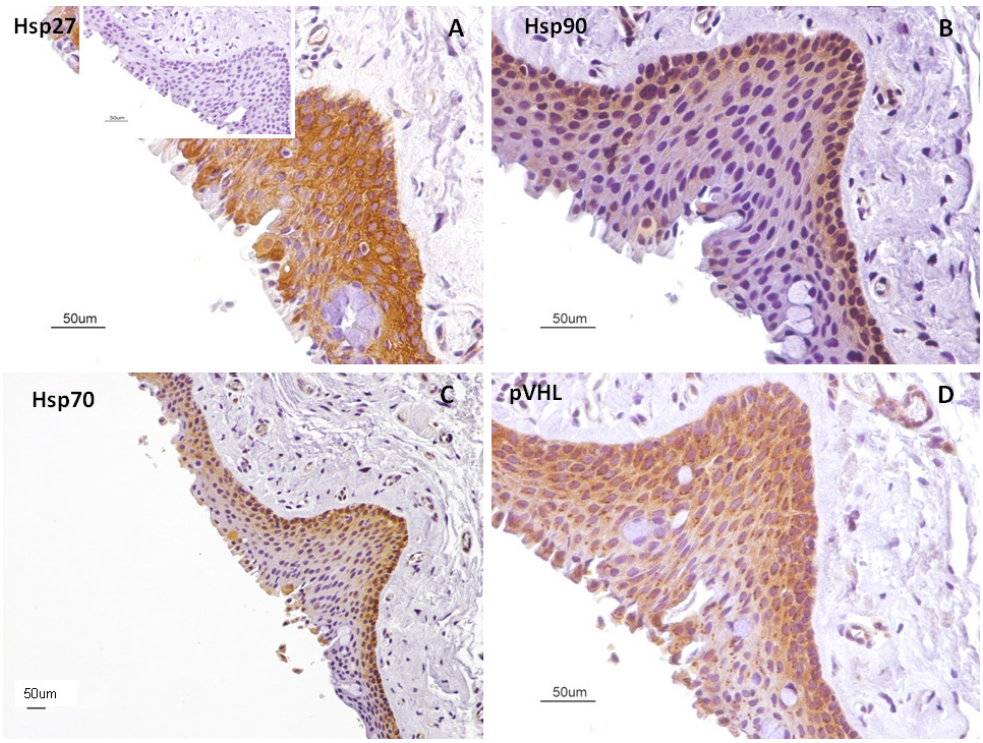

Figure 3. Panel comparing Hsps staining (**A**-**C**) and pVHL (**D**) staining in homologous fields of immediately adjacent sections of a pterygium sample. **A**: Goblet cells in the superficial layer of epithelium are Hsp27 negative whereas the remaining cells exhibit strong Hsp27 cytoplasmic immunoreactivity. Immunostaining is absent in sections incubated with control IgG (insert). **B**: Hsp90-positive cells with moderate to strong cytoplasmic immunoreactivity are distributed in basal and suprabasal layers of epithelium. **C**: Basal and suprabasal cells display moderate cytoplasmic immunoreactivity for Hsp70. **D**: The pVHL-expressing cells with strong immunoreactivity are distributed in all epithelial layers in this pterygium sample. (Dako Envision Plus Detection System with hematoxylin counterstain, original magnification X200 [**C**], X400 [**A**, **B**, **D**], bar 50 µm).

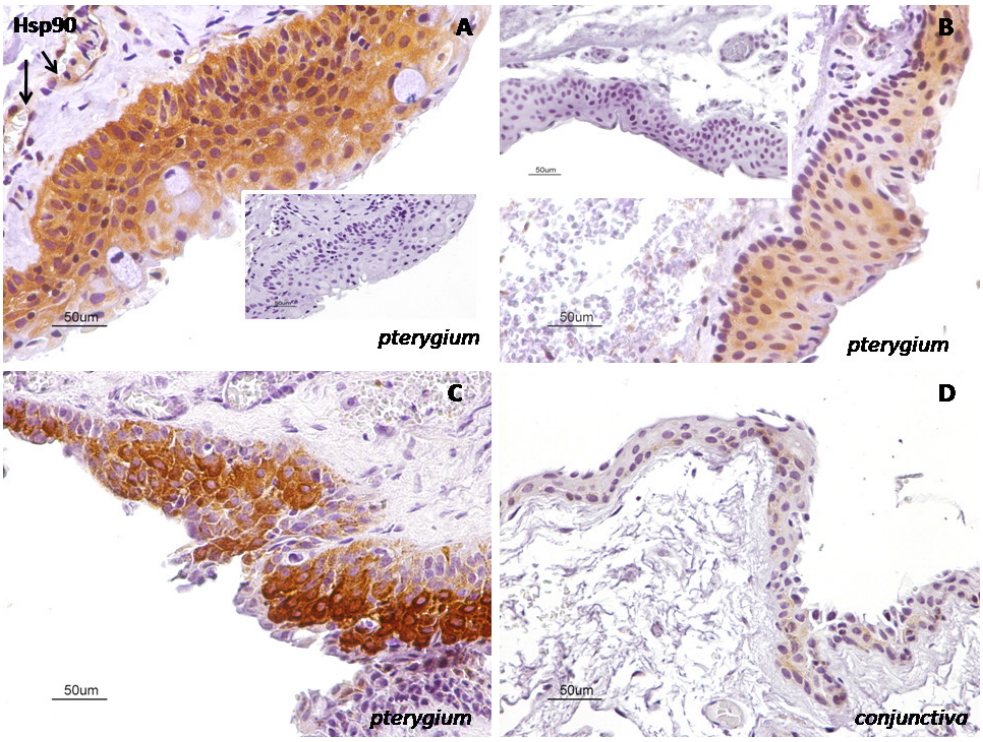

Figure 4. Panel depicting the cellular distribution of Hsp90 in pterygia (**A**-**C**) and normal conjunctiva (**D**). Note the considerable staining heterogeneity in different pterygium samples (**A**-**C**). **A**: Epithelial cells in all layers demonstrate strong Hsp90 in this pterygium sample. Arrows indicate Hsp90 positive endothelial cells. Immunostaining is absent in sections incubated with control IgG (insert). **B**: Epithelial cells with weak to moderate immunostaining patterns are distributed in all epithelial layers. Immunostaining is absent in sections incubated with control IgG (insert). **C**: Hsp90-positive cells are adjacent to Hsp90-negative cells, showing the staining heterogeneity within this pterygium sample. **D**: Epithelial cells with weak cytoplasmic immunoreactivity are detected mainly in basal and suprabasal layers in normal conjunctival samples. (Dako Envision Plus Detection System with hematoxylin counterstain, original magnification X400, bar 50 µm).

significantly higher expression of HIF-1α, Hsp27, and Hsp90 in primary pterygia (Table 4).

Expression of HIF-1α, pVHL, and Hsps by immunoblot analysis: Immunoblotting experiments on tissue extracts from pterygium and normal conjunctival samples were performed to confirm the expression of HIF-1α, pVHL, and Hsps as detected with immunohistochemistry. These experiments clearly demonstrated the presence of the expected 27 kDa band of the Hsp27 protein and also the expected 27-KDa size for its phosphorylated isoform phospho-Hsp27 in pterygia and normal conjunctiva. Similarly, expected bands of 70 kDa, and 90 kDa were found for the expression of Hsp70 and Hsp90, respectively. Immunoblots for HIF-1α exhibited a specific band at 120 kDa and multiple bands of weaker intensity at 100–120 kDa, which represent post-translational modifications of HIF-1α. No signal for HIF-1α was detected in normal conjunctival samples. Finally, for the pVHL protein, the main band was detected around 30-KDa and one additional band of weaker intensity at 14-kDa was also noted (not shown). The pVHL immunoreactive band was hardly detectable in pterygia, and similar pVHL immunoreactive bands were observed in normal conjunctival samples. A representative western blot is depicted in Figure 9A. Blot quantification showed a significant increase in expression for HIF-1α and Hsps but not for pVHL in pterygia (Figure 9B).

Co-localization of HIF-1α and Hsp90: Double immunofluorescence staining in pterygia revealed that nuclear HIF-1α expression was co-localized with cytoplasmic Hsp90 expression in cells distributed in the entire width of the epithelium (Figure 10A). In contrast, in samples where HIF-1α was detected in the cytoplasm, this expression was not co-localized with Hsp90 staining (Figure 10B); specifically, HIF-1α cytoplasmic staining was mainly observed in superficial epithelial cells whereas Hsp90 expression was limited to the basal and suprabasal epithelial cells (Figure 10C). In normal conjunctiva, double immunofluorescence showed Hsp90 expression mainly in the basal epithelial cells (Figures 10D-F) whereas HIF-1α immunoreactivity was detected in the cytoplasm of a few epithelial cells (Figure 10E,F).

DISCUSSION

HIF-1α expression is significantly increased in pterygium compared to normal conjunctiva: In this study, we investigated the co-expression patterns of HIF-1α and pVHL as well as Hsps (Hsp90, Hsp70, and Hsp27) in pterygium and normal conjunctival human samples. Accumulating experimental data reveal that HIFs (HIF-1α and HIF-2α) and their

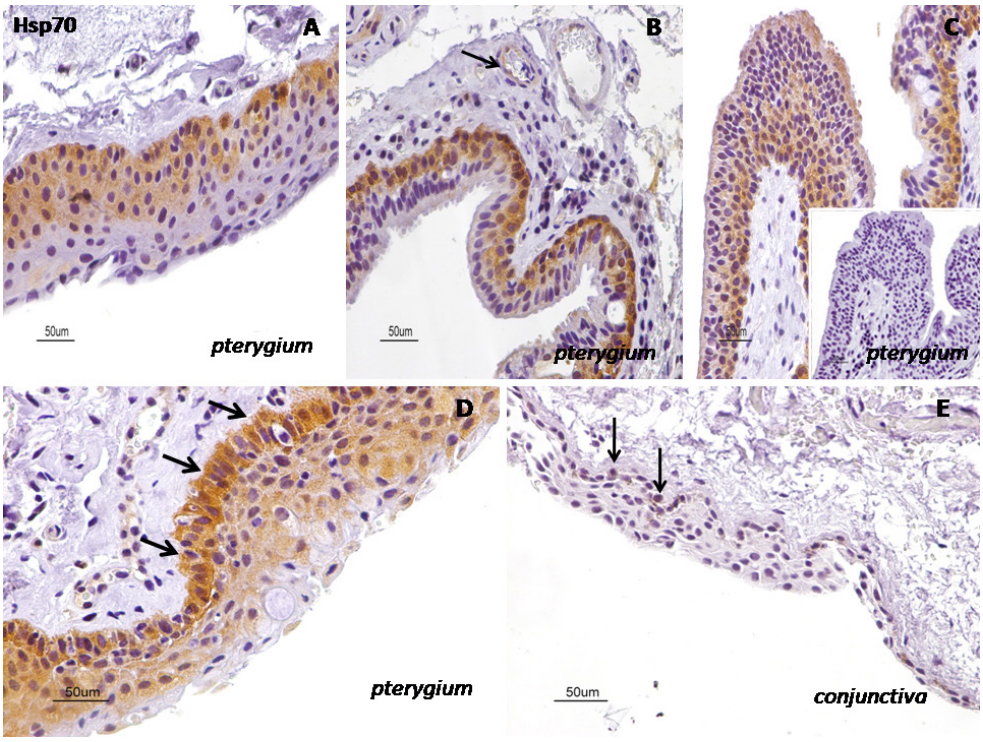

Figure 5. Panel depicting the cellular distribution of Hsp70 in pterygia (**A**-**D**) and normal conjunctiva (E). **A**: Basal and suprabasal epithelial cells display moderate cytoplasmic Hsp70 immunoreactivity. **B**: Epithelium basal and suprabasal layers and stroma vessels (arrow) are Hsp70 positive in this pterygium sample. **C**: Epithelial cells distributed in the entire epithelium show Hsp70 immunoreactivity. Immunostaining is absent in sections incubated with control IgG (insert). **D**: Basal cells exhibit more intense immunoreactivity compared to the other epithelial cells (arrows). **E**: Scattered basal epithelial cells with weak cytoplasmic immunoreactivity (arrows) are detected in normal conjunctival sample. (Dako Envision Plus Detection System with hematoxylin counterstain, original magnification X400, bar 50 µm).

target genes are master regulators of selective adaptation of cells to oxygen and nutrient deprivation [25-27]. Furthermore, the activated HIFs regulate the transcription of genes that may play a critical role in the modulation of the stemness properties of cells [51]. In this study we used immunohistochemistry to identify the enhanced expression of HIF-1α in a high percentage of pterygial epithelial cells compared to normal conjunctiva (Table 3). The localization of HIF-1α was mainly nuclear even though cytoplasmic immunoreactivity was also detected in a proportion of epithelial cells (Figure 1). Western blot analysis demonstrated HIF-1α expression in pterygia samples but not in normal conjunctiva (Figure 9B). These findings suggest that HIF-1α plays a role in the pathogenesis and growth of the pterygium lesion.

Previous studies in pterygium suggest that ocular hypoxia may exist [5,23]. As is known, hypoxia may activate the nuclear translocation of HIF-1α, resulting in its upregulation and activation [52], but overexpressed HIF-1α is also constitutively localized to the nucleus under normoxic conditions [53]. According to the Groulx and Lee model [54], nuclear translocation itself seems to be constitutive, independent of oxygen availability or pVHL status in cells infected with an adenovirus expressing GFP fused to the HIF-1α subunit. It has been proposed that the upregulation of HIF activity, even in normoxia, may be differently regulated through the sustained stimulation of growth factor and cytokine pathways [55-60]. In pterygium, ultraviolet irradiation causes the production of a variety of growth factors (e.g., EGF, TGF-beta, bFGF, HB-EGF, and IGFBP-2) [61]. These data indicate that the activation of HIF-1α in pterygium could not only be the result of hypoxia but also of hypoxia-independent mechanisms, such as oncogene activation and growth factor signaling pathways.

Additionally, HIF-1α can be activated under normoxia by loss of the von Hippel-Lindau tumor suppressor protein (which normally acts to keep levels of HIF-1α activity low) [28] or by the lack of interaction with proteins that promote its ubiquination—even if these are overexpressed—and, therefore, the nuclear translocation of HIF-1α can protect it from degradation [62]. Indeed, recent data in pterygium indicate that SAT1— a highly regulated rate-enzyme in polyamine metabolism—which is involved in the oxygen-independent degradation of HIF-1α, is abundantly expressed [21]. In the current study, we investigated the expression patterns of HIF-1α in relation to pVHL.

pVHL is consistently expressed in pterygium and normal conjunctiva and is not correlated to the HIF-1α expression: Previous data have shown that HIF-1α degradation can occur in both compartments in some specific cell types, such as

Table 3. Comparison of immunohistochemical expression of HIF-1a, pVHL, and Hsps in epithelium of pterygia and normal conjunctiva. The (non-parametric) Wilcoxon's Rank-Sum test was performed and the level of significance was defined as p<0.05.

LIs	Pterygium Mean±SD, % (range)	Normal conjunctiva Mean±SD, % (range)	*p*
HIF-1α	39.91±37.29 (1–80)	1.57±1.9 (0–2)	0.03*
pVHL	57.1±32.17 (20–100)	33.57±24.62 (0–80)	0.05
Hsp90	65.16±30.15 (5–90)	23±21.98 (0–80)	0.0029*
Hsp70	36.47±30.12 (2–80)	12.86±11.13 (0–80)	0.06
Hsp27	81.56±26.95 (15–100)	48.57±28.54 (20–80)	0.0068*

Labeling Index (LI), the percentage of positively (labeled) cells out of the total number of epithelial cells counted; Mean, mean labeling index; SD, standard deviation; * Significant difference in Labeling Indices.

primary endothelial cells (e.g., from mouse brain) [63], and that pVHL may be found in both the cytoplasm and nucleus [54,64,65]. In this study, while distinct cytoplasmic localization of pVHL was detected in pterygial epithelial cells (Figure 6), there was no significant correlation between HIF-1α and pVHL immunopositive cells (Figure 7F). Similarly, there was no significant difference in pVHL expression between pterygium and conjunctival samples as detected by immunohistochemistry (Table 3) and western blot quantification (Figure 9B). These results show that pVHL does not play a role in the degradation of HIF-1α in pterygium, indicating another possible mechanism for HIF-1α upregulation in pterygial epithelial cells.

As was mentioned, pVHL was consistently detected in both pterygium and conjunctival epithelial cells. This finding is in accordance with previous results that demonstrate a wide expression of pVHL in normal human tissues [66,67], especially in the cytoplasm of epithelial cells covering the body

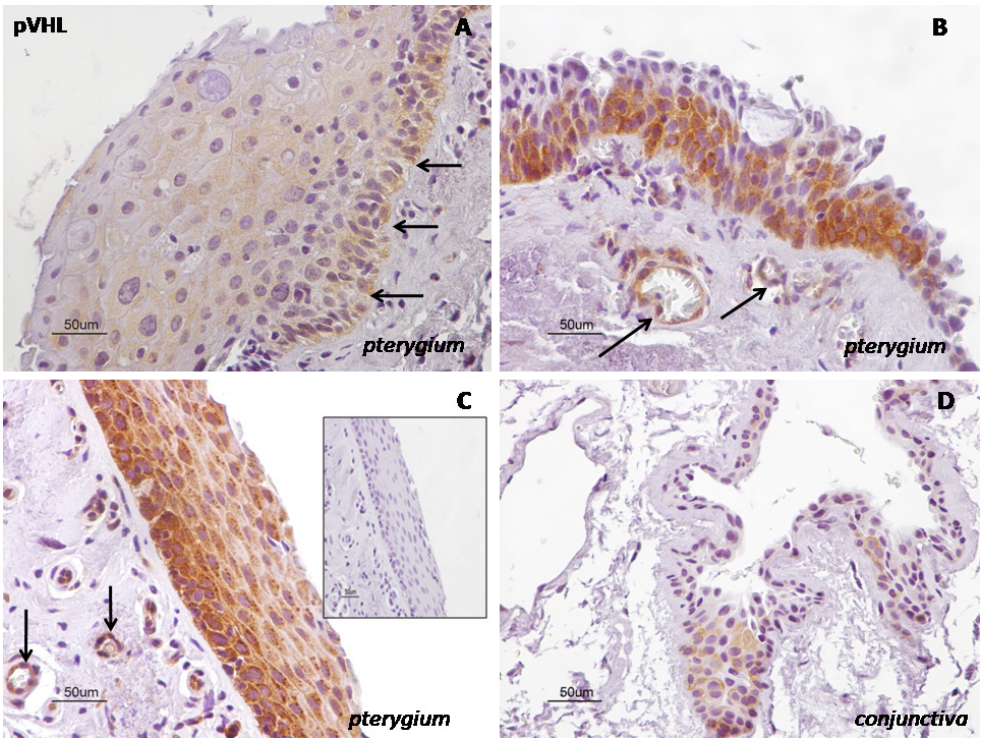

Figure 6. Panel depicting the cellular distribution of pVHL in pterygia (**A**-**C**) and normal conjunctiva (**D**). Note the considerable staining heterogeneity in different pterygium samples (**A**-**C**). **A**: Weak cytoplasmic immunoreactivity in numerous epithelial cells of pterygium tissue. Arrows show basal epithelial cells with increased staining compared to the other epithelial cells. **B**: Strong cytoplasmic immunoreactivity in basal and suprabasal cells of pterygium tissue. Arrows show pVHL positive stroma vessels. **C**: The pVHL-expressing cells with strong immunoreactivity are distributed in all epithelial layers in this pterygium sample. Arrows show pVHL-positive stroma vessels. Immunostaining is absent in sections incubated with control IgG (insert). **D**: Epithelial cells with weak cytoplasmic immunoreactivity are detected mainly in basal layer in normal conjunctival sample. (Dako Envision Plus Detection System with hematoxylin counterstain, original magnification X400, bar 50 µm).

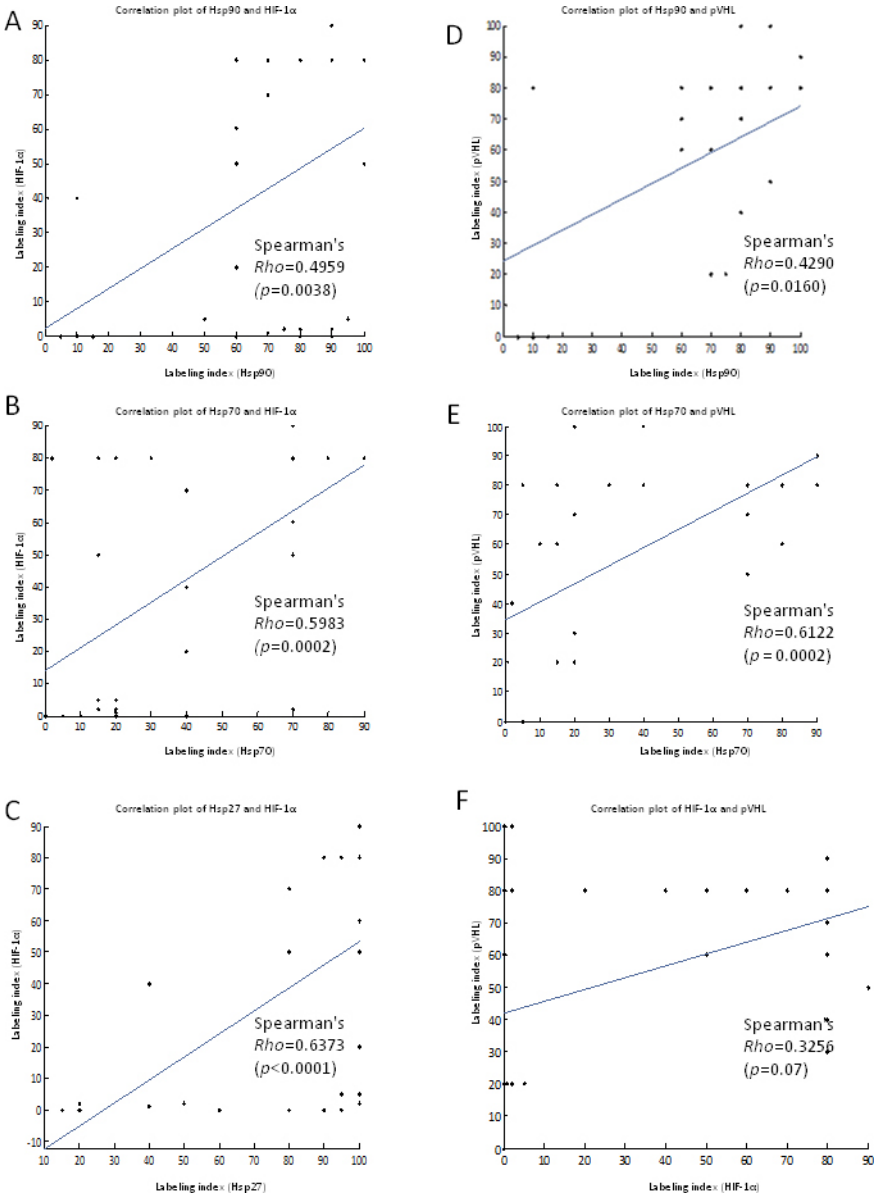

Figure 7. A highly significant relationship, between HIF-1α and Hsp LIs and between pVHL and Hsp90/Hsp70 LIs was revealed with correlation analysis. **A-C**: Scatter plot graph comparing the LIs for Hsps (Hsp90, Hsp70, and Hsp27) and HIF-1α in pterygium samples included in the study. **D, E**: Scatter plot graph comparing the LIs for Hsps (Hsp90 and Hsp70) and pVHL in pterygium samples included in the study. **F**: Scatter plot graph comparing the LIs for HIF-1α and pVHL in pterygium samples included in the study. The significance level was defined as $p<0.05$.

surface and the alimentary, respiratory, and genitourinary tracts [68]. Remarkably, pVHL strong cytoplasmic immunoreactivity was demonstrated in vessels of pterygia but not in normal conjunctiva (Figure 6). Studies of tumors have also shown expression of pVHL in endothelial cells, fibroblasts, and pericytes [68]. Thus, pVHL may be implicated in mechanisms of angiogenesis in pterygium.

Hsps are significantly increased in pterygium compared to normal conjunctiva: Previous studies have reported the existence of cross-regulation between the oxygen-sensing and heat shock pathways [36,37]. Overexpression of Hsps has been shown to demonstrate their dual roles as regulators of protein conformation as well as anti-apoptotic mediators [46,47]. Immunohistochemical data have demonstrated expression of Hsp90, Hsp70, and Hsp27 in normal conjunctival epithelium [69]. In the current study, western blot quantification revealed significantly increased protein levels of Hsp90, Hsp70, and Hsp27 (including phospho-Hsp27) in pterygia compared to normal conjunctival samples (Figure 9B). Immunohistochemically, a significantly higher percentage of immunopositive epithelial pterygial cells for Hsp90 and Hsp27 was detected in pterygia whereas the expression levels of Hsp70 did not differentiate between normal conjunctival and pterygium epithelium (Table 3). A recent study by Sebastiá et al. [70] also reported highly statistically significant differences

Table 4. Comparison of immunohistochemical expression of HIF-1a, pVHL, and Hsps in epithelium of primary and recurrent pterygia. The (non-parametric) Wilcoxon's Rank-Sum test was performed and the level of significance was defined as p<0.05.

LIs	Recurrent Pterygium Mean±SD, % (range)	Primary Pterygium Mean±SD, % (range)	*p*
HIF-1α	8.6±17.57	45.7±37.24	0.04*
pVHL	40±37.42	60.38±30.79	0.2
Hsp90	36±33.43	70.56±26.79	0.04*
Hsp70	16±15.57	40.26±30.8	0.1
Hsp27	54±29.60	86.67±23.62	0.009*

Labeling Index (LI), the percentage of positively (labeled) cells out of the total number of epithelial cells counted; Mean, mean labeling index; SD, standard deviation; * Significant difference in labeling indices.

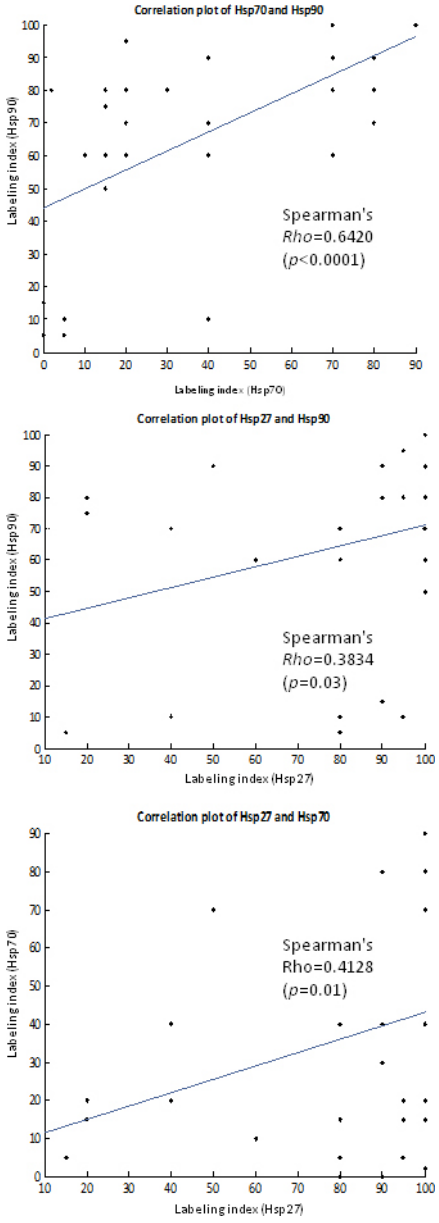

Figure 8. Expression of each Hsp was significantly correlated with the others. **A**: Scatter plot graph comparing the LIs for Hsp70 and Hsp90. **B**: Scatter plot graph comparing the LIs for Hsp27 and Hsp90. **C**: Scatter plot graph comparing the LIs for Hsp27 and Hsp70. The significance level was defined as p<0.05.

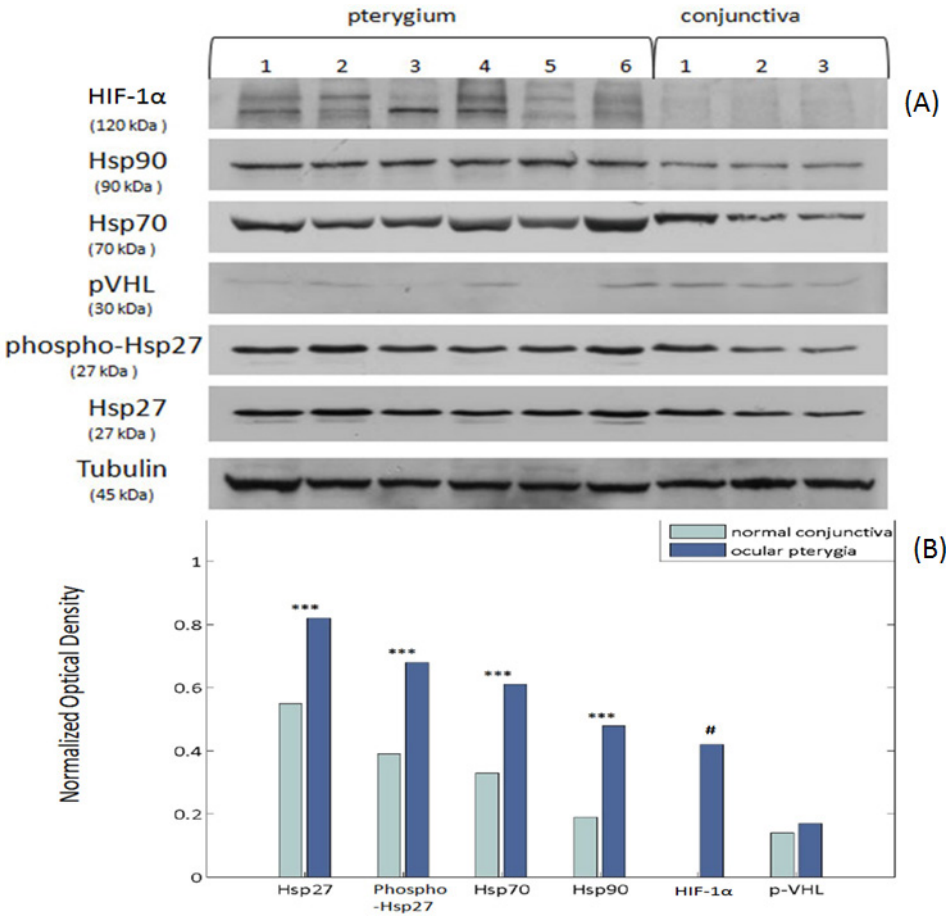

Figure 9. Immunoblot analysis of tissue extracts from pterygia and normal conjunctiva. Examination of hematoxylin and eosin-stained frozen sections from frozen tissue blocks was performed before the western blotting. **A**: The extracts probed with anti-HIF-1α (first panel), anti-Hsp90 (second panel), anti-Hsp70 (third panel), anti-pVHL (fourth panel), anti-phosphoHsp27 (fifth panel), anti-Hsp27 (sixth panel), and antibody against tubulin (bottom panel). The same amount of protein (50 µg) was loaded into each lane. Positions of molecular mass markers (in kilodaltons) are indicated on the left. The HIF-1α at 120 kDa was detected only in pterygia. Multiple bands of weaker intensity at 100–120 kDa represent post-translational modification of HIF-1α. The 90 kDa Hsp90 protein was expressed in both pterygium and normal conjunctiva samples. A 70 kDa band for Hsp70 was found in both pterygium and normal conjunctiva samples. Molecular weight of Hsp27 is 27 kDa, and its phosphorylated isoform phospho-HSP27 has been noted to be about 27 kDa. Hsp27 and phospho-Hsp27 were expressed in both pterygium and normal conjunctiva samples. For pVHL, the major band detected around the 30 kDa and one additional band of weaker intensity at 14-KDa were also noted (not shown). The pVHL-immunoreactive band was hardly detectable in pterygia, and similar pVHL-immunoreactive bands were observed for normal conjunctival samples. **B:** The corresponding densitometry analysis. The higher protein expression in pterygia compared to normal conjunctiva was statistically significant for Hsp90 (***$p<0.00001$), Hsp70 (***$p<0.00001$), and Hsp27 and phospho-Hsp27 (***$p = 0.0001$). No significant difference was detected for pVHL expression ($p = 0.3$). No statistical analysis was performed for HIF-1α expression since all pterygium samples demonstrated HIF-1α expression whereas HIF-1α was not detected in normal conjunctival samples.

in Hsp90 positive cells between normal conjunctiva and pterygium epithelium.

Hsp90 and Hsp70 were mainly detected in basal and suprabasal layers of epithelium (Figure 4, Figure 5) whereas Hsp27 was distributed in all epithelial layers of pterygia (Figure 2). Interestingly, in some pterygium samples basal epithelial cells were Hsp27-immunonegative (Figure 2C), indicating association of this protein with cell differentiation. In addition, Hsp27 has been reported to be a predifferentiation marker [71,72]. However, differences between various epithelial cell layers of pterygium have been also previously detected, with p53 expression being higher in basal cells compared to more superficial layers [73].

Not surprisingly, analysis of Hsp expression patterns revealed that each Hsp was significantly correlated with the others (Figure 8). Furthermore, Hsp90 and Hsp70 were significantly correlated with the expression of pVHL in pterygial epithelial cells (Figure 7D,E). Interestingly, expression of Hsps (Hsp90, Hsp70, and Hsp27) was also detected in endothelial cells in pterygia but not in normal conjunctiva, indicating a possible role of these proteins in angiogenesis of pterygium. These findings suggest that, in pterygium, finely tuned interactions between Hsps and their co-chaperones and client proteins mediate the cytoprotective actions of Hsps against stress. However, as it has been proposed for tumors, it is possible that the accumulation of Hsps may contribute to

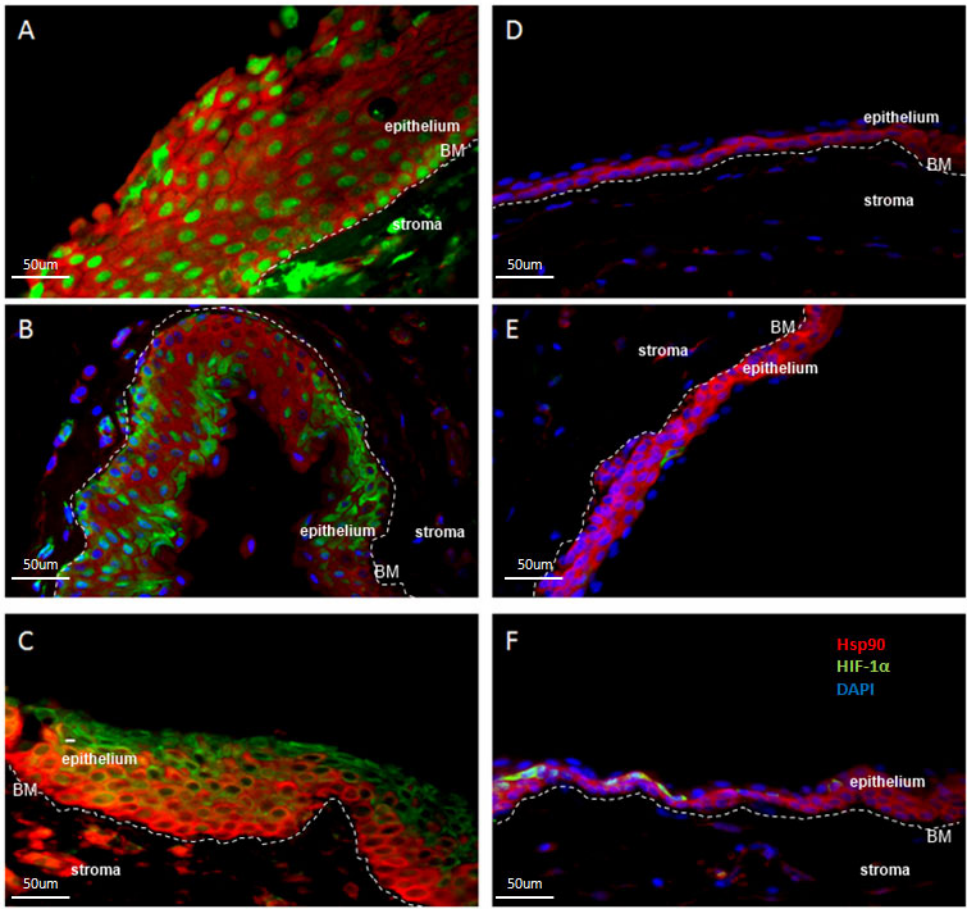

Figure 10. Distribution of HIF-1α (green) and Hsp90 (red) as determined by double immunofluorescence staining in pterygia (**A-C**) and normal conjunctiva samples (**D-F**). Nuclei are DAPI labeled in blue. **A**: Co-localization of HIF-1α nuclear expression with Hsp90 cytoplasmic expression in cells of the entire epithelium. **B**: Hsp90 is absent from focally distributed cells with cytoplasmic HIF-1α immunoreactivity. **C**: Cytoplasmic staining of HIF-1α is demonstrated in superficial layers of epithelium whereas Hsp90 staining is limited to basal and suprabasal layers. **D-F**: Conjunctival basal epithelial cells demonstrate Hsp90 cytoplasmic immunoreactivity. **E, F**: A few HIF-1α positive cells with cytoplasmic staining are clearly detectable. The dashed line indicates the pterygium basement membrane (BM). The scale bar represents 50 µm.

many of the traits that permit the malignant phenotype [44]. Notably, it has recently been shown that Hsp90 plays a critical role in the pathogenesis of conjunctival melanoma [74].

Expression of HIF-1α is correlated to the expression of Hsps in pterygial epithelial cells: In this study, an analysis of HIF-1α and Hsp expression patterns was performed. It is known that HIF-1α can bind to the promoters of all Hsp genes in response to stress [38]. A strong relationship between HIF-1α expression and Hsps (Hsp90, Hsp70, and Hsp27) expression levels was found (Figure 7A-C), indicating that there may be cross-regulation between HIF-1α and HSF in pterygia as a result of the effort of the cells to protect themselves under stressful conditions. Functional studies will clarify whether the upregulation of the Hsps in pterygia is derived exclusively from the HIF-1α activation.

Hsp90 is co-localized with HIF-1α in pterygial epithelial cells: Hsp90, co-operating with Hsp70, appears to be more specialized to capture client proteins involved in cell signaling, such as transcription factors and protein kinases [45]. Previous data show that Hsp90, acting as a molecular chaperon, stabilizes the HIF-1α in renal carcinoma cell lines while disruption of HIF-1α/Hsp90 promotes the ubiquitination and proteasome-mediated degradation of HIF-1α in an oxygen- and pVHL-independent manner and diminishes HIF-1α transcriptional activity [32].

In this study, we used double immunofluorescence staining to show co-localization of HIF-1α and Hsp90 in pterygial epithelial cells. Specifically, nuclear HIF-1α was co-localized with Hsp90 cytoplasmic expression. On the contrary, cytoplasmic HIF-1α expression was not co-localized with Hsp90 expression (Figure 10). These findings lend support to the hypothesis that Hsp90 plays a critical role in the stabilization of HIF-1α and its subsequently nuclear translocation in pterygium. As a result, the transcriptional activity of HIF-1α is strongly promoted.

HIF-1α and Hsp expression is differentiated between primary and recurrent pterygia: Studies have shown that primary and recurrent pterygia are quite different. In particular, the morphology of recurrent pterygium is different, and its prognosis is worse. Tong et al. [22] suggested that recurrence is a distinct biologic phenomenon from the formation of primary pterygium. According to their findings, the recurrence of

pterygium may be related to an imbalance of growth signals rather than due to mere prolongation of the stimulus that initiated the primary pterygia formation. Indeed, elevated expression of HIF-1α, pVHL, and Hsps was observed in recurrent pterygia compared to normal conjunctiva (Table 4), confirming the view of Tong et al. [22] regarding the formation of recurrent pterygium. Moreover, Tong et al. [22] hypothesized that a low level of inflammation plays a critical role in recurrence of a pterygium. Considering the accumulating data implicating HIF in the regulation of immunity and inflammation [75] as well as data reporting the induction of Hsps because of inflammation [42], it is logical to speculate that HIF-1α and Hsps may be involved in the pathogenesis of recurrent pterygium.

Notably, Tong et al. [22] reported that genes with increased expression are not the same in both primary and recurrent pterygium. In contrast, we immunohistochemically demonstrated that the significantly increased genes in recurrent pterygium are the same as those that increased in primary pterygium epithelial cells compared to normal conjunctiva. Specifically, significantly increased expression for HIF-1α, Hsp90, and Hsp27 was detected in primary compared to recurrent pterygium epithelia. These findings enhance the importance of the role of cross-regulation of HIF-1α and Hsps in the development of pterygium and highlight the hypothesis of Tong et al. [22] that the differentiation in protein expression is likely associated with differences in pathogenesis between the two pterygium types. Thus, HIF-1α and Hsps appear to be implicated in the formation not only of primary but also of recurrent pterygium, probably through different signaling pathways.

In summary, the results of the current study suggest that, in pterygium, HIF-1α upregulation is independent from pVHL expression but dependent on hypoxia and/or hypoxia-independent mechanisms. Furthermore, since the most prevalent hypothesis for the pathogenesis of pterygium is that focal limbal irradiation of corneal epithelial stem cells causes alteration of these cells and a breakdown of the limbal barrier [9,11], the upregulation of activated HIF-1α in pterygium may represent an adaptive process for the survival of stem/progenitor as well as non-stem cells under stressful conditions. The complete eradication of these cells, by targeting the HIF signaling network, might be beneficial in the therapeutic approach to pterygia. Further trials will evaluate the role of HIF-1α and Hsps coordinated activation in pterygium pathogenesis and treatment.

ACKNOWLEDGMENTS

The authors kindly thank Professor F. Angelatou, PhD, Department of Physiology, School of Medicine, University of Patras, for her support in this study, and Assoc. Professor S. Taraviras, PhD, Department of Physiology, School of Medicine, University of Patras, for providing the immunofluorescence microscope. The technical contributions by K. Botsakis, PhD, and M. Spella, PhD, Department of Physiology, School of Medicine, University of Patras, in the Western and Immunofluorescence analysis, respectively, are gratefully acknowledged.

REFERENCES

1. Hilgers JH. Pterygium: its incidence, heredity and etiology. Am J Ophthalmol 1960; 50:635-44. [PMID: 13714249].
2. Duke-Elder S, ed. Diseases of the Outer Eye Part 1. System of Ophthalmology 8. London: Kimpton; 1965. p. 569- 585.
3. Chan CM, Liu YP, Tan DT. Ocular surface changes in pterygium. Cornea 2002; 21:38-42. [PMID: 11805505].
4. Austin P, Jakobiec FA, Iwamoto T. Elastodysplasia and elastodystrophy as the pathologic bases of ocular pterygia and pinguecula. Ophthalomology 1983; 90:96-109. [PMID: 6828309].
5. Seifert P, Sekundo W. Capillaries in the epithelium of pterygium. Br J Ophthalmol 1998; 82:77-81. [PMID: 9536887].
6. Marcovich AL, Morad Y, Sandbank J, Huszar M, Rosner M, Pollack A, Herbert M, Bar-Dayan Y. Angiogenesis in pterygium: morphometric and immunohistochemical study. Curr Eye Res 2002; 25:17-22. [PMID: 12518239].
7. Aspiotis M, Tsanou E, Gorezis S, Ioachim E, Skyrlas A, Stefaniotou M, Malamou-Mitsi V. Angiogenesis in pterygium: study of microvascular density, vascular endothelial growth factor, and thrombospondin-1. Eye (Lond) 2007; 21:1095-101. [PMID: 16823458].
8. Liu L, Yang D. Immunological studies on the pathogenesis of pterygium. Chin Med Sci J 1993; 8:84-8. [PMID: 8292805].
9. Coroneo MT, Di Girolamo N, Wakefield D. The pathogenesis of pterygia. Curr Opin Ophthalmol 1999; 10:282-8. [PMID: 10621537].
10. Detorakis ET, Spandidos D. Pathogenetic mechanisms and treatment options for ophthalmic pterygium: Trends and perspectives Int J Mol Med 2009; 23:439-47. Review[PMID: 19288018].
11. Kwok LS, Coroneo MT. A model for pterygium formation. Cornea 1994; 13:219-24. [PMID: 8033571].
12. Dushku N, Reid TW. Immunohistochemical evidence that human pterygia originate from an invasion of vimentin-expressing altered limbal epithelial basal cells. Curr Eye Res 1994; 13:473-81. [PMID: 7924411].

13. Chui J, Coroneo MT, Tat LT, Crouch R, Wakefield D, Di Girolamo N. Ophthalmic pterygium: a stem cell disorder with premalignant features. Am J Pathol 2011; 178:817-27. [PMID: 21281814].

14. Sevel D, Sealy R. Pterygia and carcinoma of the conjunctiva. Trans Ophthalmol Soc U K 1969; 88:567-78. [PMID: 5272278].

15. Perra MT, Colombari R, Maxia C, Zucca I, Piras F, Corbu A, Braavo S, Scarpa A, Sirigu P. Finding of conjunctival melanocytic pigmented lesions within pterygium. Histopathology 2006; 48:387-93. [PMID: 16487360].

16. Hirst LW, Axelsen RA, Schwab I. Pterygium and associated ocular surface squamous neoplasia. Arch Ophthalmol 2009; 127:31-2. [PMID: 19139334].

17. Chen JK, Tsai RJ, Lin SS. Fibroblasts isolated from human pterygia exhibit transformed cell characteristics. In Vitro Cell Dev Biol Anim 1994; 30A:243-8. [PMID: 7520809].

18. Jing Y, Han Z, Zhang S, Liu Y, Wei L. Epithelial-mesenchymal transition in tumor microenvironment. Cell Biosci 2011; 1:29-[PMID: 21880137].

19. Kato N, Shimmura S, Kawakita T, Miyashita H, Ogawa Y, Yoshida S, Higa K, Okano H, Tsubota K. Beta-catenin activation and epithelial-mesenchymal transition in the pathogenesis of pterygium. Invest Ophthalmol Vis Sci 2007; 48:1511-7. [PMID: 17389479].

20. Dushku N, John MK, Schultz GS, Reid TW. Pterygia pathogenesis: corneal invasion by matrix metalloproteinase expressing altered limbal epithelial basal cells. Arch Ophthalmol 2001; 119:695-706. [PMID: 11346397].

21. Jaworski CJ, Aryankalayil-John M, Campos MM, Fariss RN, Rowsey J, Agarwalla N, Reid TW, Dushku N, Cox CA, Carper D, Wistow G. Expression analysis of human pterygium shows a predominance of conjunctival and limbal markers and genes associated with cell migration. Mol Vis 2009; 15:2421-34. [PMID: 19956562].

22. Tong L, Chew J, Yang H, Ang LPK, Tan DTH, Beuerman RW. Distinct gene subsets in pterygia formation and recurrence: dissecting complex biological phenomenon using genome wide expression data. BMC Med Genomics 2009; 2:14-[PMID: 19272163].

23. Lee JK, Song YS, Ha HS, Park JH, Kim MK, Park AJ, Kim JC. Endothelial progenitor cells in pterygium pathogenesis. Eye (Lond) 2007; 21:1186-93. [PMID: 16732212].

24. Kase S, Osaki M, Jin X-H, Ohgami K, Yoshida K, Saito W, Takahashi S, Nakanishi K, Ito H, Ohno S. Increased expression of erythropoietin receptor in human pterygial tissues. Int J Mol Med 2007; 20:699-702. [PMID: 17912463].

25. Wenger RH. Cellular adaptation to hypoxia: O2-sensing protein hydroxylases, hypoxia-inducible transcription factors, and O2-regulated gene expression. FASEB J 2002; 16:1151-62. [PMID: 12153983].

26. Huang LE, Bunn HF. Hypoxia-iducible factor and its biomedical relevance. J Biol Chem 2003; 278:19575-8. [PMID: 12639949].

27. Semenza GL. Regulation of oxygen homeostasis by hypoxia-inducible factor 1. Physiology (Bethesda) 2009; 24:97-106. [PMID: 19364912].

28. Ohh M, Park CW, Ivan M, Hoffman MA, Kim TY, Huang LE, Pavletich N, Chau V, Kaelin WG. Ubiquitination of hypoxia-inducible factor requires direct binding to the beta-domain of the von Hippel-Lindau protein. Nat Cell Biol 2000; 2:423-7. [PMID: 10878807].

29. Frew IJ, Krek W. Multitasking by pVHL in tumour suppression. Curr Opin Cell Biol 2007; 19:685-90. [PMID: 18006292].

30. Zhang Q, Yang H. The roles of VHL-dependent ubiquitination in signaling and cancer. Front Oncol 2012; 2:35-[PMID: 22649785].

31. Maxwell PH, Wiesener MS, Chang GW, Clifford SC, Vaux EC, Cockman ME, Wykoff CC, Pugh CW, Maher ER, Ratcliffe PJ. The tumor suppressor protein VHL targets hypoxia-inducible factors for oxygen-dependent proteolysis. Nature 1999; 399:271-5. [PMID: 10353251].

32. Isaacs JS. Jung Y-J, Mimnaugh EG, Martinez A, Cuttitta F, Neckers LM. Hsp90 regulates a von Hippel Lindau-independent hypoxia-inducible factor-1α-degradative pathway. J Biol Chem 2002; 277:29936-44. [PMID: 12052835].

33. Mabjeesh NJ, Post DE, Willard MT, Kaur B, Van Meir EG, Simons JW, Zhong H. Geldanamycin induces degradation of hypoxia-inducible factor 1 alpha protein via the proteosome pathway in prostate cancer cells. Cancer Res 2002; 62:2478-82. [PMID: 11980636].

34. Liu YV, Baek JH, Zhang H, Diez R, Cole RN, Semenza GL. RACK1 competes with HSP90 for binding to HIF-1α and is required for O_2-independent and HSP90 inhibitor-induced degradation of HIF-1a. Mol Cell 2007; 25:207-17. [PMID: 17244529].

35. Kim W-Y, Oh SH, Woo J-K, Hong WK, Lee H-Y. Targeting heat shock protein 90 overrides the resistance of lung cancer cells by blocking radiation-induced stabilization of hypoxia-inducible factor 1α. Cancer Res 2009; 69:1624-32. [PMID: 19176399].

36. Baek SH, Lee UY, Park EM, Han MY, Lee YS, Park YM. Role of protein kinase Cdelta in transmitting hypoxia signal to HSF and HIF-1. J Cell Physiol 2001; 188:223-35. [PMID: 11424089].

37. Baird NA, Turnbull DW, Johnson EA. Induction of the heat shock pathway during hypoxia requires regulation of heat shock factor by hypoxia-inducible factor-1. J Biol Chem 2006; 281:38675-81. [PMID: 17040902].

38. Calderwood SK, Xie Y, Wang X, Khaleque MA, Chou SD, Murshid A, Prince T, Zhang Y. Signal transduction pathways leading to heat shock transcription. Sign Transduct Insights 2010; 2:13-24. [PMID: 21687820].

39. Trautinger F, Kindås-Mügge I, Knobler RM, Hönigsmann H. Stress proteins in the cellular response to ultraviolet radiation. J Photochem Photobiol B 1996; 35:141-8. [PMID: 8933720].

40. Multhoff G. Heat shock proteins in immunity. Handbook Exp Pharmacol 2006; 172:279-304. [PMID: 16610364].

41. Kalmar B, Greensmith L. Induction of heat shock proteins for protection against oxidative stress. Adv Drug Deliv Rev 2009; 61:310-8. [PMID: 19248813].

42. Jones Q, Voegeli TS, Li G, Chen Y, Currie RW. Heat shock proteins protect against ischemia and inflammation through multiple mechanisms. Inflamm Allergy Drug Targets 2011; 10:247-59. [PMID: 21539516].

43. Morange M. HSFs in development. Handbook Exp Pharmacol 2006; xx:153-69. [PMID: 16610359].

44. Ciocca DR, Arrigo AP, Calderwood SK. Heat shock proteins and heat shock factor 1 in carcinogenesis and tumor development: an update. Arch Toxicol 2013; 87:19-48. [PMID: 22885793].

45. Jakob U, Buchner J. Assisting spontaneity: the role of Hsp90 and small Hsps as molecular chaperons. Trends Biochem Sci 1994; 19:205-11. [PMID: 7914036].

46. Mosser DD, Morimoto RI. Molecular chaperons and the stress of oncogenesis. Oncogene 2004; 23:2907-18. [PMID: 15077153].

47. Garrido C, Brunet M, Didelot C, Zermati Y, Schmitt E, Kroemer G. Heat shock proteins 27 and 70. Anti-apoptotic proteins with tumorigenic properties. Cell Cycle 2006; 5:2592-601. [PMID: 17106261].

48. Ciocca DR, Calderwood SK. Heat shock proteins in cancer: diagnostic, prognostic, predictive, and treatment implications. Cell Stress Chaperones 2005; 10:86-103. [PMID: 16038406].

49. Altman DG. Practical statistics for medical research. London: Chapman and Hall; 1991.

50. Kudo A, Fukushima H, Kawakami H, Matsuda M, Goya T, Hirano H. Use of serial semithin frozen sections to evaluate the co-localization of estrogen receptors and progesterone receptors in cells of breast cancer tissues. J Histochem Cytochem 1996; 44:615-20. [PMID: 8666746].

51. Mimeault M, Batra SK. Hypoxia-inducing factors as master regulators of stemness properties and altered metabolism of cancer- and metastasis-initiating cells. J Cell Mol Med 2013; 17:30-54. [PMID: 23301832].

52. Kallio PJ, Okamoto K, O'Brien S, Carrero P, Makino Y, Tanaka H, Poellinger L. Signal transduction in hypoxic cells: inducible nuclear translocation and recruitment of the CBP/p300 coactivator by the hypoxia-inducible factor-1α. EMBO J 1998; 17:6573-86. [PMID: 9822602].

53. Hofer T, Desbaillets I, Höpfl G, Gassmann M, Wenger RH. Dissecting hypoxia-dependent and hypoxia-independent steps in the HIF-1α activation cascade: implications for HIF-1α gene therapy. FASEB J 2001; 15:2715-7. [PMID: 11606485].

54. Groulx I, Lee S. Oxygen-dependent ubiquitination and degradation of hypoxia inducible factor requires nuclear-cytoplasmic trafficking of the von Hippel-Lindau tumor suppressor protein. Mol Cell Biol 2002; 22:5319-36. [PMID: 12101228].

55. Stroka DM, Burkhardt T, Desbaillets I, Wenger RH, Neil DA, Bauer C, Gassmann M, Candinas D. HIF-1 is expressed in normoxic tissue and displays an organspecific regulation under systemic hypoxia. FASEB J 2001; 15:2445-53. [PMID: 11689469].

56. Richard DE, Berra E, Pouyssegur J. Nonhypoxic pathway mediates the induction of hypoxia-inducible factor 1alpha in vascular smooth muscle cells. J Biol Chem 2000; 275:26765-71. [PMID: 10837481].

57. Pagé EL, Robitaille GA, Pouysségur J, Richard DE. Induction of hypoxia-inducible factor-1alpha by transcriptional and translational mechanisms. J Biol Chem 2002; 277:48403-9. [PMID: 12379645].

58. Zhou J, Brüne B. Cytokines and hormones in the regulation of hypoxia inducible factor-1alpha (HIF-1alpha). Cardiovasc Hematol Agents Med Chem 2006; 4:189-97. [PMID: 16842205].

59. Lauzier MC, Pagé EL, Michaud MD, Richard DE. Differential regulation of hypoxia-inducible factor-1 through receptor tyrosine kinase transactivation in vascular smooth muscle cells. Endocrinology 2007; 148:4023-31. [PMID: 17510240].

60. Kuschel A, Simon P, Tug S. Functional regulation of HIF-1α under normoxia–is there more than post-translational regulation? J Cell Physiol 2012; 227:514-24. [PMID: 21503885].

61. Di Girolamo N, Chui J, Coroneo MT, Wakefield D. Pathogenesis of pterygia: role of cytokines, growth factors, and matrix metalloproteinases. Prog Retin Eye Res 2004; 23:195-228. [PMID: 15094131].

62. Berchner-Pfannschmidt U, Frede S, Wotzlaw C, Fandrey J. Imaging of the hypoxia-inducible factor pathway: insights into oxygen sensing. Eur Respir J 2008; 32:210-7. [PMID: 18591338].

63. Zheng X, Ruas JL, Cao R, Salomons FA, Cao Y, Poellinger L, Pereira T. Cell-type-specific regulation of degradation of hypoxia-inducible factor 1a: role of subcellular compartmentalization. Mol Cell Biol 2006; 26:4628-41. [PMID: 16738327].

64. Lee S, Chen DY, Humphrey JS, Gnarra JR, Linehan WM, Klausner RD. Nuclear/cytoplasmic localization of the von Hippel-Lindau tumor suppressor gene product is determined by cell density. Proc Natl Acad Sci USA 1996; 93:1770-5. [PMID: 8700833].

65. Karhausen J, Kong T, Narravula S, Colgan SP. Induction of the von Hippel-Lindau tumor suppressor gene by late hypoxia limits HIF-1 expression. J Cell Biochem 2005; 95:1264-75. [PMID: 15962286].

66. Los M, Jansen GH, Kaelin WG, Lips CJ, Blijham GH, Voest EE. Expression pattern of the von Hippel-Lindau protein in human tissues. Lab Invest 1996; 75:231-8. [PMID: 8765323].

67. Corless CL, Kibel AS, Iliopoulos O, Kaelin WG Jr. Immunostaining of the von Hippel-Lindau gene product in normal

and neoplastic human tissues. Hum Pathol 1997; 28:459-64. [PMID: 9104946].

68. Sakashita N, Takeya M, Kishida T, Stackhouse TM, Zbar B, Takahashi K. Expression of von Hippel-Lindau protein in normal and pathological human tissues. Histochem J 1999; 31:133-44. [PMID: 10416685].

69. Berra A, Dutt JE, Nouri M, Foster CS. Heat shock protein expression in human conjunctiva. Invest Ophthalmol Vis Sci 1994; 35:352-7. [PMID: 8112980].

70. Sebastiá R, Ventura MP, Solari HP, Antecka E, Orellana ME, Burnier MN Jr. Immunohistochemical detection of Hsp90 and Ki-67 in pterygium. Diagn Pathol 2013; 8:32-[PMID: 23432803].

71. Parcellier A, Brunet M, Schmitt E, Col E, Didelot C, Hammann A, Nakayama K, Nakayama KI, Khochbin S, Solary E, Garrido C. HSP27 favors ubiquitination and proteasomal degradation of p27Kip1 and helps S-phase reentry in stressful cells. FASEB J 2006; 20:1179-81. [PMID: 16641199].

72. Mehlen P, Mchlen A, Godet J, Arrigo AP. Hsp27 as a switch between differentiation and apoptosis in murine embryonic stem cells. J Biol Chem 1997; 272:31657-65. [PMID: 9395507].

73. Tan DT. Lim As, Goh HS, Smith DR. Abnormal expression of the p53 tumor suppressor gene in the conjunctiva of patients with pterygium. Am J Ophthalmol 1997; 123:404-5. [PMID: 9063255].

74. Westekemper H, Karimi S, Süsskind D, Anastassiou G, Freistühler M, Steuhl KP, Bornfeld N, Schmid KW, Grabellus F. Expression of HSP 90, PTEN and Bcl-2 in conjunctival melanoma. Br J Ophthalmol 2011; 95:853-8. [PMID: 20956280].

75. Scholz CC, Taylor CT. Targeting the HIF pathway in inflammation and immunity. Curr Opin Pharmacol 2013; 13:646-53. [PMID: 23660374].

Articles are provided courtesy of Emory University and the Zhongshan Ophthalmic Center, Sun Yat-sen University, P.R. China. The print version of this article was created on 30 March 2014. This reflects all typographical corrections and errata to the article through that date. Details of any changes may be found in the online version of the article.